POAC'13
Espoo, Finland

Proceedings of the 22nd International Conference on
Port and Ocean Engineering under Arctic Conditions
June 9-13, 2013
Espoo, Finland

NUMERICAL SIMULATIONS OF SHEAR PROPERTIES OF ICE RUBBLE: A SHEAR BOX EXPERIMENT

Aniket Patil[1,2], Bjørnar Sand[2] , Lennart Fransson[1]

[1]Luleå University of Technology, Luleå, SWEDEN.
[2]Northern Research Institute, Narvik, NORWAY.

ABSTRACT

Ice rubble has highly nonlinear behavior and thus simulate shear properties requires sophisticated constitutive models including a relatively large number of parameters and complicated calibration procedures. An attempt has been made to simulate shear properties of ice rubble. A shear box experiment is chosen from test series performed by Fransson and Sandkvist (1985). In this paper a shear box test is simulated with nonlinear finite element code LS-Dyna. A newly implemented material model in LS-Dyna called continuous surface cap model (CSCM) has been used in this simulation. This model is proposed by Schwer and Murray (1994). For the sake of simplicity, experimental results are compared with Mohr-Coulomb material model. A brief overview of continuous surface cap model is given. Finally, comparisons with experimental results have been made.

INTRODUCTION

Finding first year ice ridge rubble properties are of great interest since activities of exploration and production of hydrocarbons in arctic area increased. Design load level of offshore structures in arctic and sub-arctic area depends on first year ridge properties. Ice ridges are composed of consolidated and unconsolidated parts. In unconsolidated parts rubble exists in two different forms. In sail, rubble is usually dry and voids are comprised of air and slush between the blocks. In keel, rubble is wet, consisting of brine pockets and voids are comprised of water, slush and loose blocks.

The number of contact points in the rubble decreases with increasing block size. Pressure in each point reaches to crushing strength of ice. Crushing leads to milled ice packs with several block sizes and an increased number of contact points. As a result, distinct gliding plane will develop when shear forces are applied. The smaller ice pieces may act like roller bearings for the bigger blocks and small pieces may also be compacted to become bigger mass. Ettema and Urroz (1989) stated that rubble undergoing continuous deformation is cohesionless. Laboratory tests offer greater insights of rubble deformations under prescribed boundary and loading conditions. In reality ice rubble constantly evolves during life time of ridge. rubble deformation procedure can be described as initial, main and decay phase (Høyland, 2002, Høyland and Liferov, 2005). Laboratory tests on ice rubble are normally conducted during the initial phase, which is believed to be the most sensitive with respect to the testing conditions. Scaling laws between the prototype and the model is of high significance when performing laboratory tests on ice rubble (Liferov, 2005).

Many researchers have performed extensive experimental studies dedicated to finding ice rubble properties. Out of all laboratory tests, shear box tests have been used extensively for ice rubble because of its simplicity and easy to perform attribute. The shear box test is a laboratory experiment usually performed to get shear properties of material under some confinement load. There are limited numbers of choices available when it comes to simulate pressure dependent materials like ice rubble. Being a two parametric model, the Mohr-Coulomb material model was used because of its simplicity and reasonable accuracy. In this paper, a shear box test is simulated in nonlinear finite element code LS-Dyna with two different material models Mohr-Coulomb and continuous surface cap model CSCM. This continuous surface cap model has been developed and implemented into LS-Dyna (Model no 159) by Schwer and Murray (1994). Results from simulations are discussed and compared with experiments.

SHEAR BOX EXPERIMENT

Experimental setup

Fransson and Sandkvist (1985) performed a series of shear box tests on brash ice. The main purpose of the test series was to present results from laboratory tests with different types of ice and to discuss the shear properties of fresh water ice based on these tests. Brash ice is a material that becomes more resistant to shearing as it is squeezed more tightly by normal pressure.

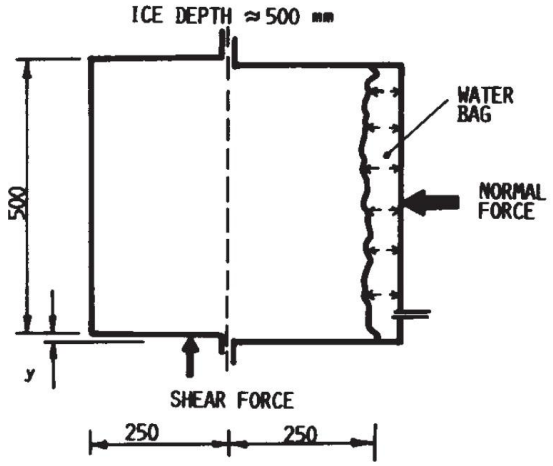

Figure 1.sketch showing the shear box with the water bag for keeping constant normal forces from Fransson and Sandkvist (1985).

Figure 1 shows the general setup of the shear box test they used. A box of 13 mm thick board was used to form a cubical space of 0.5 x 0.5 x 0.5 m into two halves. The confinement pressure was applied in the range of 0-8 kPa from side with help of a water bag supported by board. Due to inertia force of the system, the normal pressure is varied with normal displacement of moving part of box. The shearing force and the displacement of the moving part were recorded. The moving speed of one halve of box was close to a mean value of 10 mm/s while the other half of box was fixed. A gap between two parts was 6 mm. As the top was open, rubble pieces could move upwards. Discussed test series were performed under isothermal conditions with no freezing or melting effects.

Ice rubble properties

These test series were performed with ice rubble made of three different types of ice. But tests performed with ice no 3 are subject of interest, so only those properties are given here. An ice cover of 50 mm thickness was produced by cold seeding at -20° C. The average columnar ice grain size was 3 mm. This type of rubble was produced by crushing ice sheets frozen in a laboratory basin. The form of the ice pieces changes from broken sheets with sharp edges to more spherical forms due to shearing. The rubble was produced with mean block sizes of 110 mm. The block sizes and distribution are not scaled to actual cases. These tests can be seen as small scale tests.

Results from tests

Results are interpreted by identifying different shear modes as discussed by Hellmann (1984). Various authors have showed that higher freeze bond strength gives higher shear stress (Serré, Repetto-Llamazares et al., 2011). There is also different explanation available for each shear mode. Results from Fransson and Sandkvist (1985) using ice no. 3 have been chosen for this simulation.

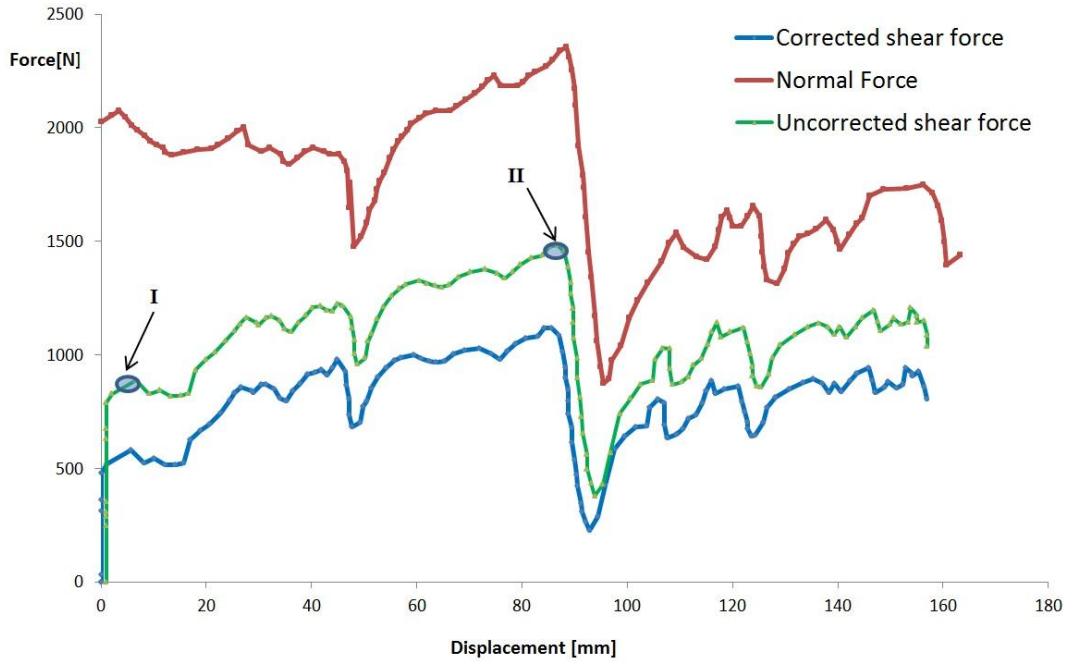

Figure 2. Test results clearly showing shear modes from Fransson and Sandkvist (1985).

Additionally, the measured shear force should be corrected due to friction of the box, which was recorded as 9°. In Figure 2 corrected graph is recalculated. Corrected shear force is calculated as given below

$$F_{corr} = F_{\exp} - N\tan(9^{\circ}). \quad (1)$$

As shown in Figure 2 the first shear mode (I) corresponds to rearrangement of blocks resulting in denser packing and gliding plane. The second mode (II) occurs at maximum shear forces before failure. Linear increase (hardening) in the shear force with displacement between first and

second shear mode represents smaller failure, local crushing and rearrangements of the ice rubble. Fransson and Sandkvist (1985) further analyzed the data to estimate internal angle of friction (φ) for both the peak. They estimated for first shear mode φ is 12° and for second shear mode φ is 14°. The reason they give for such a low values of internal friction angle is presence of higher content of fine grained ice.

FINITE ELEMENT MODEL

A simplified finite element model is created based on the experiment description given by Fransson and Sandkvist, 1985. The ice rubble is modelled by solid element having shape of 500 mm cube (shown in green colour). One fixed part and one moving part (bracket) modelled with solid element. A constant normal pressure of 8 kPa is applied at the open side (shown by blue arrow) while top side is free. The bracket is moved at constant speed of 10 mm/s (direction is shown by red arrow in Figure 3). Static (0.08) and dynamic (0.04) coefficient of friction is applied between rubble and side walls as well as bottom surface. A gravity force is applied to the rubble.

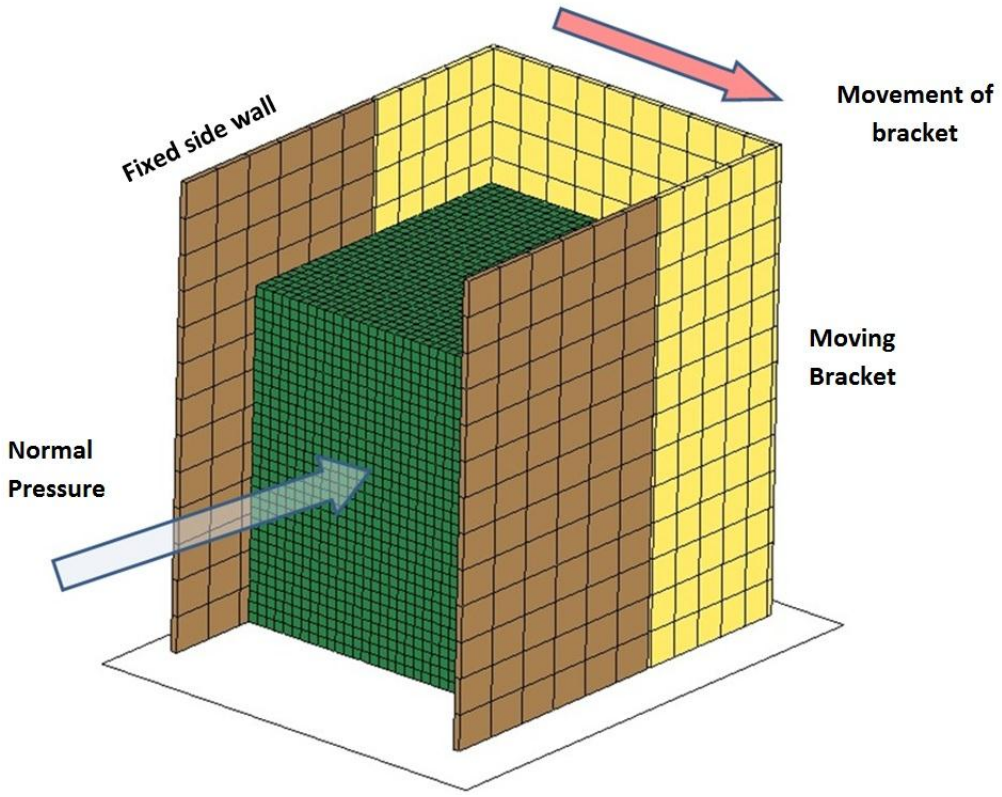

Figure 3. Finite element model of shear box experiment.

Mesh size (15.6 mm) is selected based on response to force displacement time curve and computational time. As orientation of rubble relative to box cannot always be anticipated as the model undergoes large deformations, an automatic surface to surface is selected as contact algorithm between box walls and rubble. This contacts check for penetration on either

side of an element (Hallquist, 2006). The maximum displacement of box is 150 mm. In order to simulate such a large displacement, walls were made higher to support rubble movement.

MATERIAL MODELS

Mohr-Coulomb (LS-Dyna Material Model 173)

Mohr Coulomb theory gives linear relationship between normal stress and shear stress. The model gives a straight forward connection between the shear strength and the material parameters (internal angle of friction and cohesion). However rubble behavior is not linear over a wide range of stress-strain space. Mohr-Coulomb always predicts higher strength and does not consider softening. There are computational difficulties with this model, as the yield envelope contains corners in the stress space therefore the MC model is not robust in numerical finite element analysis without any modification. Formulation is given below as

$$\tau_{\max} = c + \sigma_n \tan\varphi. \qquad (2)$$

where τ_{max} and σ_n are the maximum shear and normal stresses on the failure surface respectively, φ is the angle of internal friction and c is the cohesion. Linear elastic and ideal plastic type of material formulation of Mohr-Coulomb is used for this simulation.

Continuous surface cap model (CSCM) (LS-Dyna Material Model 159)

This material model originally developed to predict dynamic performance, elastic and plastic deformation and failure of concrete. In this simulation it is used to simulate ice rubble's different failure modes. The general shape of the yield surface in meridonal plane is shown in Figure 4. This surface uses a multiplicative formulation to combine the shear failure surface with the isotropic hardening compaction cap surface smoothly and continuously. The smooth intersection eliminates the numerical complexity of treating a corner region between the failure surface and cap (Murray, 2007).

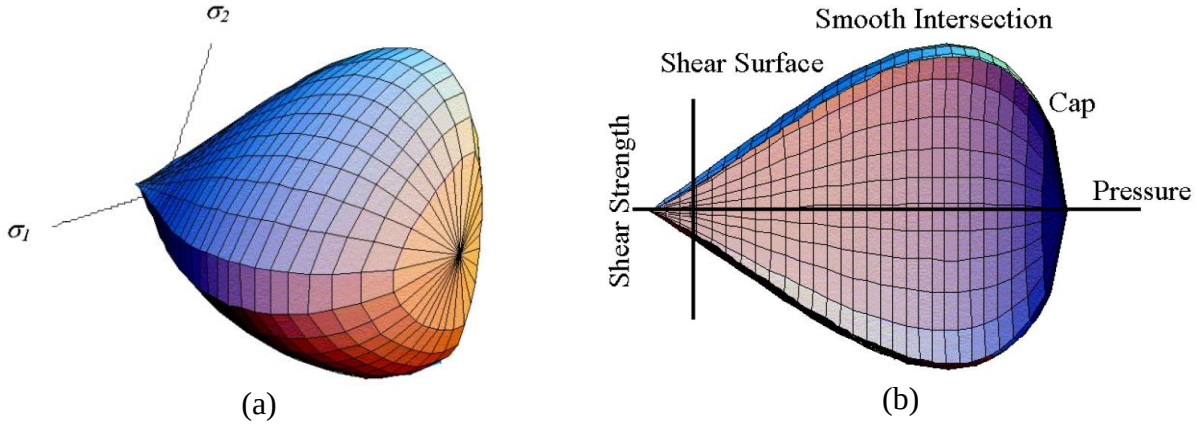

Figure 4. General shape of the CSCM model yield surface in three dimensions (a) and in two dimensions (b) in meridonal plane (from Murray, 2007)

This smooth cap surface provides reduction in CPU time and advantage over numerical

instability. The present model provides a further extension in which the standard functional dependence of the failure and cap surfaces on the first and second stress invariants is expanded to include the third stress invariant. Introduction of the third stress invariant allows simultaneous fitting of the model to triaxial compressive data and triaxial extension data (Schwer and Murray, 1994). The failure surface of the smooth cap model is defined as

$$F_f(J_1) = \alpha - \lambda \exp^{-\beta J_1} + \theta J_1 \ .$$
$$J_1 = 3P \ . \tag{3}$$

where J_1 is the first invariants of the stress tensor, P is mean stress and α, θ, λ, β and are model parameters used to match the triaxial compression and are fixed at λ=0, β =0.

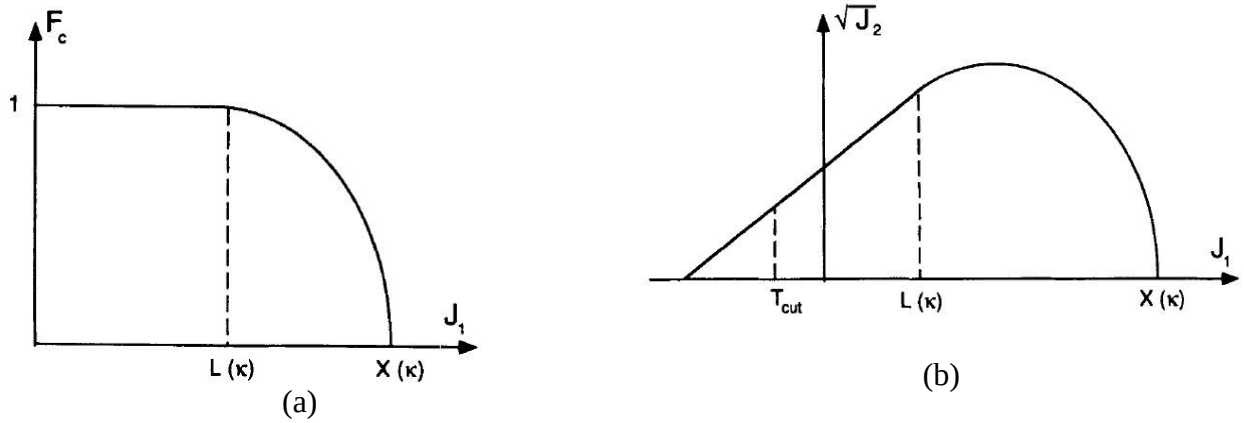

(a) (b)

Figure 5. (a) Non-dimensional function used for cap portion of the smooth cap model function. (b) Single smooth cap failure function (from Schwer and Murray, 1994)

The isotropic hardening or cap surface of the model is based on a non-dimensional functional form, given below

$$F_c(J_1, \kappa) = 1 - \frac{\left[J_1 - L(\kappa)\right]\left[\left|J_1 - L(\kappa)\right| + J_1 - L(\kappa)\right]}{2\left[X(\kappa) - L(\kappa)\right]^2} \ . \tag{4}$$

where κ is a hardening parameter that controls the motion of the cap surface and L(κ) and X(κ) define the geometry of the cap surface. The smooth cap model, shown in Figure 5 (b), is formed by multiplying together the failure and hardening surface functions to form a smoothly varying function given by

$$f(J_1, J_2^{'}, \kappa) = J_2^{'} - F_f^2 . F_C \ . \tag{5}$$

Where $J_2^{'}$ is the second invariant of the deviatoric stress tensor.
The evolution of cap's motion is defined by the isotropic hardening rule

$$\varepsilon_v^p = W(1 - e^{-D_1(X - X_0) - D_2(X - X_0)^2}) \ . \tag{6}$$

where ε_v^p is the plastic volumetric strain, W is the maximum plastic volumetric strain, X_0 is the initial intercept of the cap surface and D_1 and D_2 are the linear and quadratic shape parameters

respectively. D_1 and D_2 determine the shape of the pressure volumetric strain curves. W determines the maximum plastic volume compaction.

The five input parameters (X_0, W, D_1, D_2, and R) have to be selected from fits to the pressure-volumetric strain curves in isotropic compression and uniaxial strain. 'R' is cap aspect ratio, 'X_0' determines the pressure at which compaction initiates in isotropic compression. 'R' combined with 'X_0' , determines the pressure at which compaction initiates in uniaxial strain. In addition to inclusion of the standard isotropic hardening of the cap surface, the present model includes kinematic hardening of shear surface. Although kinematic hardening is usually introduced to model the Bauschinger effect, this implementation is based on tri axial compression data which shows hardening of the initial shear yield surface. Hardening of the rubble can be observed in between first and second shear mode (see Figure 2). CSCM requires defining two more additional parameters (N_H and C_H) to define the yield surface initial location and subsequent motion. N_H defines the initial location of yield surface and C_H defines the hardening rate of yield surface.

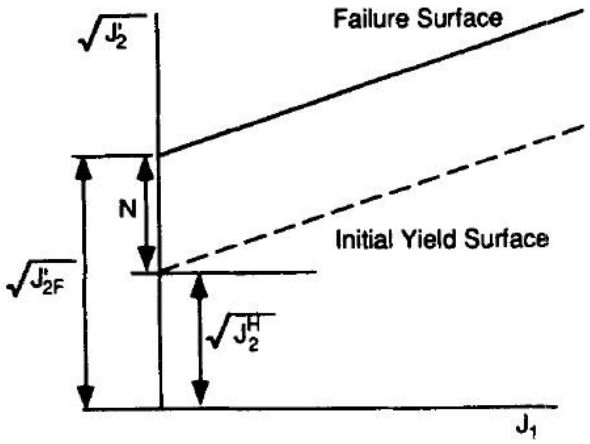

Figure 6. Original failure surface and translating yield surface

Figure 6 shows the working of N_H where $J_2^{'}$ is second invariant of the deviatoric stress tensor and $J_{2F}^{'}$ is final location yield surface whereas J_2^H is initial k location yield surface. In case of kinematic hardening formulation modifies the shear surface definition, as given below

$$F_f(J_1) = N_H(\alpha - \lambda \exp^{-\beta J_1} + \theta J_1). \tag{7}$$

where N_H is hardening initiation or initial location and C_H is hardening rate. Detailed formulation can be found in Schwer and Murray (1994).

PARAMETERS USED IN SIMULATION

Out of 21 parameter to be selected for CSCM, some of the parameters are based on a parametric study and some are kept at default value. To obtain all the parameters by experimentation a large experiment data base is needed. So some of the parameters are calculated based on a sensitive study. Given below is the explanation of the selection procedure.

Stiffness

Based on experimental data available, Young's modulus (E) has been selected to 100 MPa and shear modulus (G) and bulk modulus (K) are calculated based on following relationship

$$G = \frac{E}{2(1+\upsilon)} \quad , \quad K = \frac{E}{3(1-2\upsilon)} \tag{8}$$

where ν is Poisson's ratio and is selected as 0.3. Density of rubble (ρ) is used as 690 kg/m^3, G = 38.4 MPa, K=83.3 MPa.

Cohesion c

Cohesion has been back-calculated based on first shear mode and two parametric expressions of Mohr-Coulomb criteria, shown in equation (2). Based on calculation 2.7 kPa is the lowest value of cohesion that rubble can have. As described by Fransson and Sandkvist (1985), all tests were performed under isothermal conditions with no freezing or melting. Therefore, there is less time available to form any kind of cohesion. Cohesion value used in this simulation is 3 kPa.

Internal angle of friction φ and yield surface parameters

Angle of internal friction has been reported as 12° (Fransson and Sandkvist, 1985). Originally developed for concrete, material model CSCM has been validated based on extensive experiments by Schwer and Murray (1994). From analytical analysis of this curve fitting to triaxial compression data, shear failure parameters can be derived based on Mohr-Coulomb failure surface parameters as given below

$$\alpha = \frac{6c.\cos\phi}{\sqrt{3}(3-\sin\phi)} \quad , \quad \theta = \frac{2.\sin\phi}{\sqrt{3}(3-\sin\phi)} \tag{9}$$

Calculated values of α and θ are 6.083 x 10^{-3} and 14.3676 x 10^{-2} , respectively.
Other values to define yield surface based on triaxial compression , deviatoric state of torsion (TOR) and triaxial extension are fixed at λ=0, β =0 , α_1=0.7373 , θ_1= 0, λ_1=0.17, β_1=0, α_2=0.66, θ_2=0, λ_2=0.16 and β_2 =0.

Shear surface hardening

Initial shear surface can be scaled using $N_{H.}$ Figure 6 and equation 7, shows working of N_H. Murray (2007) has given upper and lower bound of values for N_H. Based on these values N_H has been selected as 0.7. To select $C_{H,}$ a single element study has been performed and it was set to 1. Damage and rate effect parameters were not used to simulate for this test.

Cap geometry and hardening

Table 1 gives cap geometry and hardening parameters used in simulation. These material parameters were determined in an iterative manner from the laboratory material response data. As given by Heinonen (2004), rubble becomes soft during the shearing process, while the shearing causes dilatation and the rubble becomes looser. Hardening or softening of the material depends

only on the volumetric plastic strain. After parametric study and basic routine optimization, these values found to be appropriate.

Table 1. Cap geometry and hardening parameters

Parameter	Value
Cap aspect ratio (R)	9.44
Initial location of cap (X_0)	0.093
Maximum plastic volume compaction (W)	0.46
linear and quadratic shape parameters D_1 and D_2	1 and 0 resp.

SIMULATION RESULTS

A force displacement graph obtained from these two material models is then compared with experimental result. Figure 7 shows force displacement graph obtained after simulating 150 mm displacement of bracket. Although, after 80 mm of displacement the rubble is extruded out of box. So results cannot be considered valid after that. Continuous expansion of rubble under shear causes higher confinement force than in experiment.

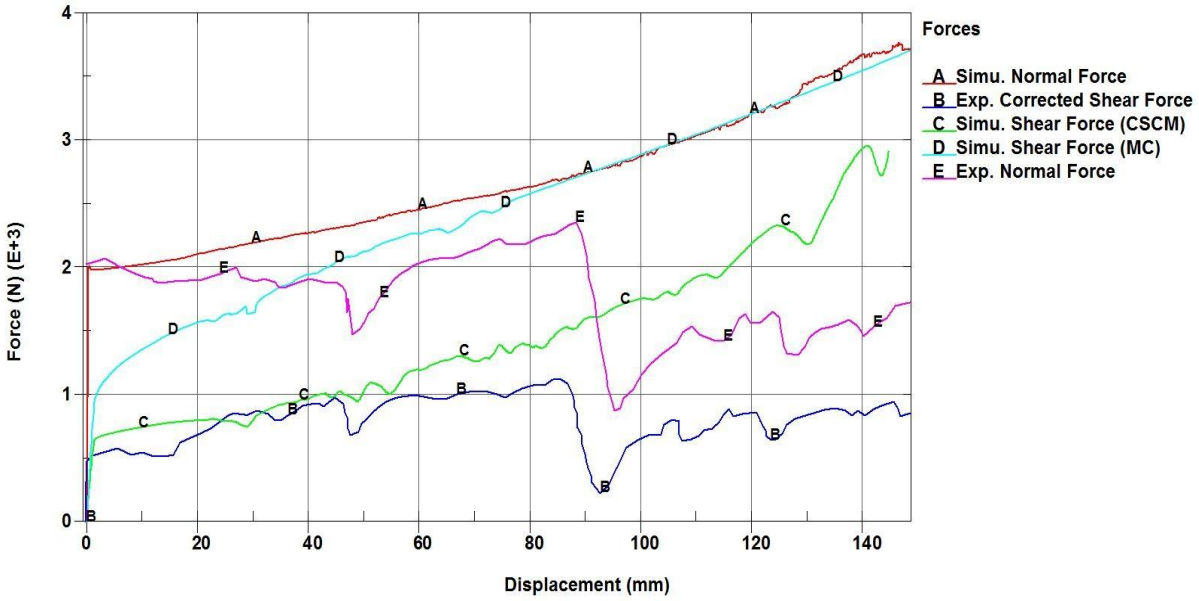

Figure 7. Comparison of force displacement graphs obtained from different material models to corrected shear force obtained from Fransson and Sandkvist (1985).

Unlike experiment setup, a constant normal pressure is applied from side and no movement is allowed of rubble in opposite direction of force. This causes additional pressure buildup.

CONCLUSION

Shear box experiment data can be analyzed based on shear modes. As discussed earlier, first peak (I)(in Figure 2) corresponds to rearrangement of block, brakeage of freeze bond leads to denser packing. Hence rubble exhibits hardening. Initial slope of experiment curve matches with simulation curves, which means that the assumption of Young's modulus (E=100 MPa) is reasonable. Mohr-Coulomb material model gives much higher first shear mode whereas CSCM gives lower first shear mode.

However, this is not the case for second shear mode. As rubble expansion was expanding linearly, there was no distinct second shear mode observed. There has been considerable difference between simulated and experimental confinement pressure. Excessive hardening observed in simulation using Mohr-coulomb for rubble can be explained by simultaneous yielding of elements in the shear zone. Hardening observed between two shear modes, have been simulated in fairly good agreement by CSCM up till 60 mm displacement of box. Expansion of rubble during the shearing process can be explained by higher dilation.

ACKNOWLEDGEMENT

This work was supported by the Research Council of Norway project number 195153.

REFERENCES

Ettema, R. and Urroz, G. E. (1989). On internal friction and cohesion in unconsolidated ice rubble. Cold Regions Science and Technology 16(3): 237-247.

Fransson, L. and Sandkvist, J. (1985). Brash ice shear properties : laboratory tests. The 8th International Conference on Port and Ocean Engineering Under Arctic Conditions : proceedings Narssarssuaq, Greenland, Dansk hydraulisk institut.

Hallquist, J. O. (2006). LS-DYNA Theoretical Manual. Livermore, Ca, Livermore Software Technology Corporation.

Heinonen, J. (2004). Constitutive modeling of ice rubble in first-year ridge keel. VTT Technical Research Centre of Finland. Publications. Espoo, Finland, . PhD Thesis: 3-142.

Hellmann, J. H. (1984). Basic investigations on mush ice. Proc. of IAHR, 7th Int. Symposium on Ice, Hamburg, Germany.

Høyland, K. V. (2002). Consolidation of first-year sea ice ridges. Journal of geophysical research 107(C6): 3062.

Høyland, K. V. and Liferov, P. (2005). On the initial phase of consolidation. Cold Regions Science and Technology 41(1): 49-59.

Liferov, P. (2005). First-year ice ridge scour and some aspects of ice rubble behaviour. Trondheim, Norway, Norwegian University of Science and Technology, Faculty of Engineering Science and Technology, Department of Civil and Transport Engineering. PhD Thesis.

Murray, Y. D. (2007). Users manual for concrete material model 159, APTEK, Inc, 1257 lake plaza drive, colorado springs, CO 80906: 89.

Schwer, L. E. and Murray, Y. D. (1994). A three-invariant smooth cap model with mixed hardening. International Journal for Numerical and Analytical Methods in Geomechanics 18(10): 657-688.

Serré, N., Repetto-Llamazares, A. H. V., et al. (2011). Experiments on the relations between freeze bond and ice rubble strength part I : shear box experiments. Port and ocean engineering under arctic conditions, Montreal, Canada.